

# Excess hemoglobin digestion and the osmotic stability of *Plasmodium falciparum*-infected red blood cells

Virgilio L. Lew, Teresa Tiffert, and Hagai Ginsburg

During their asexual reproduction cycle (about 48 hours) in human red cells, *Plasmodium falciparum* parasites consume most of the host cell hemoglobin, far more than they require for protein biosynthesis. They also induce a large increase in the permeability of the host cell plasma membrane to allow for an increased traffic of nutrients and waste products. Why do the parasites digest hemoglobin in such excess? And how can infected red cells retain their integrity for the duration of the asexual cycle when comparably permeabilized uninfected cells hemolyse earlier? To address these questions we

encoded the multiplicity of factors known to influence host cell volume in a mathematical model of the homeostasis of a parasitized red cell. The predicted volume changes were subjected to thorough experimental tests by monitoring the stage-related changes in the osmotic fragility of infected red cell populations. The results supported the model predictions of biphasic volume changes comprising transient shrinkage of infected cells with young trophozoites followed by continuous volume increase to about 10% lower than the critical hemolytic volume of approximately 150 fL by the end of the asexual

cycle. Analysis of these results and of additional model predictions demonstrated that the osmotic stability of infected red cells can be preserved only by a large reduction in impermeant solute concentration within the host cell compartment. Thus, excess hemoglobin consumption represents an essential evolutionary strategy to prevent the premature hemolysis of the highly permeabilized infected red cell. (Blood. 2003;101:4189-4194)

© 2003 by The American Society of Hematology

## Introduction

During their intraerythrocytic phase, *Plasmodium falciparum* parasites grow and divide within the red blood cells to occupy about 16- to 20-fold the volume of the invading merozoite. The parasite ingests and digests about 70% of the host cell hemoglobin (Hb)<sup>1</sup> but uses only up to 16% of the released amino acids for protein biosynthesis.<sup>2</sup> The excess is discharged out of the infected red blood cells (IRBCs) to the surrounding plasma<sup>3</sup> mainly through new permeation pathways (NPPs) of broad solute selectivity induced by the parasite in the host cell membrane.<sup>4-6</sup> The reason why parasites expend so much energy ingesting and digesting excess hemoglobin<sup>7-10</sup> and detoxifying the cell from toxic ferriprotophyrin IX<sup>11-13</sup> remains puzzling.

Another unresolved puzzle concerns the mechanism by which parasitized red cells are able to retain their osmotic stability for the approximately 48-hour reproductive cycle of the parasite despite the rapid NPP-mediated dissipation of the Na<sup>+</sup> and K<sup>+</sup> gradients.<sup>14</sup> A recent study by Staines et al<sup>15</sup> demonstrated that if NPPs were induced in *uninfected* cells as they are in infected cells, the *uninfected* cells would hemolyse by approximately 44 hours. Since the additional volume of the parasite was excluded from their computations, their estimates make the lysis resistance of IRBCs with large internal parasites even harder to comprehend.

To investigate these issues we developed a mathematical model of the homeostasis of a parasitized red cell, formulated critical predictions on the stage-related volume changes of IRBCs, and

carried out experimental tests to determine the validity of the model. The experimental results confirmed the predicted stage-related volume changes, and validated the model-based suggestion that NPP-mediated permeability and excess Hb consumption are fine-tuned to ensure the osmotic stability and integrity of the parasitized cell for the duration of its asexual cycle.

## Materials and methods

### Preparation of cells and determination of the osmotic fragility distribution of infected red cell populations

Red cells infected with *P falciparum* A4 clone (kind gift from B. C. Elford, Institute of Molecular Medicine, Oxford, United Kingdom), derived from the ITO4 line<sup>16</sup> were cultured under a low oxygen atmosphere by standard methods.<sup>17</sup> The culture medium, changed daily, was RPMI 1640 supplemented with 40 mM HEPES (*N*-2-hydroxyethylpiperazine-*N'*-2-ethanesulfonic acid), 25 mg/L gentamicin sulfate, 10 mM D-glucose, 2 mM glutamine, and 8.5% vol/vol pooled human serum. There were 9 experiments carried out, 6 with IRBCs harvested from nonsynchronized cultures and 3 from synchronized cultures. Synchronization was performed by alternating sorbitol lysis<sup>18</sup> and gelatin flotation<sup>19,20</sup>; the last synchronization was performed at least 24 hours prior to the experiment. A final gelatin flotation procedure was carried out immediately before each experiment to separate top (containing mostly IRBCs) and bottom (containing mostly uninfected cohort cells) cell fractions. The cells recovered from each

From the Physiological Laboratory, University of Cambridge, Cambridge, United Kingdom; and the Department of Biological Chemistry, Institute of Life Sciences, The Hebrew University of Jerusalem, Jerusalem, Israel.

Submitted August 29, 2002; accepted January 8, 2003. Prepublished online as *Blood* First Edition Paper, January 16, 2003; DOI 10.1182/blood-2002-08-2654.

Supported by grants 061269 and 059725 from the Wellcome Trust (United Kingdom).

**Reprints:** V. L. Lew, Department of Physiology, University of Cambridge, Downing Street, Cambridge CB2 3EG, United Kingdom; e-mail: vl11@cam.ac.uk.

The publication costs of this article were defrayed in part by page charge payment. Therefore, and solely to indicate this fact, this article is hereby marked "advertisement" in accordance with 18 U.S.C. section 1734.

© 2003 by The American Society of Hematology

fraction were washed 3 times at room temperature by centrifugation and resuspension in serum-free culture medium without phenol red. Samples were taken for estimates of parasitemia and differential cell count on thin, Giemsa-stained smears, as reported before.<sup>21</sup> After the washes, the cell pellets from top and bottom fractions were resuspended in the same medium at hematocrits of 10% and 5%, respectively, to partially compensate for their different Hb. Aliquots were then transferred to grooved plastic containers. Aliquots (10  $\mu$ L) were aspirated into 12-channel pipettes and delivered into the rows of round-bottom 96-well microplates containing 250  $\mu$ L lysis media per well, as described in the legend of Figure 3. The plates were centrifuged at 1200g for 5 minutes. Using multichannel pipettes, 150  $\mu$ L supernatant from each well was transferred to corresponding wells of flat-bottom microwell plates for measurement of Hb by Soret band absorption spectroscopy ( $\lambda = 415$  nm) in a microplate reader (Molecular Devices, Sunnyvale, CA).<sup>22</sup> The residual supernatant from selected wells was discarded and the cell pellet resuspended in RPMI for the preparation of thin blood smears and microscopic evaluation of the identity of cells that did not lyse. Preliminary trials showed that the time interval between sampling the cells into the lysing media and the centrifugation step to separate the unlysed cells from the supernatants had no detectable effects on the appearance of the hemolysis curves for at least 30 minutes. Thus, at least for this time interval, IRBCs swollen to sublytic levels remain homeostatically stable at room temperatures, just like uninfected RBCs, suggesting that the only relevant factor in hypo-osmotic-induced IRBC lysis is for the cell to reach its critical hemolytic volume.

### Mathematical model of the homeostasis of *P. falciparum*-infected red cells (HCM)

The HCM was derived from the original Lew-Bookchin red cell model,<sup>23</sup> which is available, with instructions, from <http://www.physiol.cam.ac.uk/staff/lew/index.htm>. We outline here only the specific modifications introduced in the formulation of the HCM. The maximal period of time for any simulation was set to 48 hours, the mean duration of the asexual life cycle of the parasite within its red cell host. Within this period the parasite digests host Hb, increases in volume, and induces a large increase in host plasma membrane permeability through NPPs. Although many other transport and metabolic processes take place in the parasite-host-medium system, those which determine the overall homeostatic behavior of IRBCs are essentially 3: Hb digestion, NPP-mediated traffic of the major permeant ions ( $\text{Cl}^-$ ,  $\text{Na}^+$  and  $\text{K}^+$ ), and parasite volume growth. The measured amino acid efflux from IRBCs with mature trophozoites was 13.5 nmol ( $10^8$  cells) $^{-1}\text{min}^{-1}$ , equivalent to about 80 mmol/(L cells) $^{-1}\text{hour}^{-1}$ .<sup>3</sup> The amino acid composition of the effluent was indistinguishable from that of globin suggesting that NPP permeability was high enough not to limit the rate of exit of the lesser permeable amino acids.<sup>6</sup> Because amino acid efflux was measured near the time when the rate of amino acid production from Hb was maximal,<sup>2</sup> efflux must have been even then limited by production, not permeability. This suggests that amino acid production poses no osmotic stress to the host and has thus been left out of the model, an exclusion additionally justified by the results obtained in the present study.

The equations used to model stage-related Hb consumption (H) and NPP-mediated permeabilities ( $\text{NPP}_K$ ) as a function of time were of the form  $Y = Y_{\max}/\{1 + \exp[(t - t_{1/2})/s]\}$  (Figure 1), where Y represents either Y(H) or Y( $\text{NPP}_K$ ),  $Y_{\max}$  sets the limiting value of  $H_{\max}$  or  $\text{NPP}_{K-\max}$  at a time (t) approaching 48 hours,  $t_{1/2}$  is the time taken to reach  $H_{\max}/2$  or  $\text{NPP}_{K-\max}/2$ , and s determines the slope. This 3-parameter equation provides a good fit of the patterns of Hb digestion and NPP development reported by Krugliak et al<sup>2</sup> and Staines et al,<sup>15</sup> respectively. The reason to use  $\text{NPP}_K$ , the  $\text{K}^+$  permeability through the NPP pathway, as the only function to represent the NPP-mediated ionic traffic relevant to IRBC homeostasis, is because the  $\text{Na}^+$  and  $\text{Cl}^-$  permeabilities,  $\text{NPP}_{\text{Na}}$  and  $\text{NPP}_{\text{Cl}}$ , respectively, can be directly derived from it, as established by Staines et al<sup>15</sup> and by Kirk et al.<sup>24</sup> Thus,  $\text{NPP}_{\text{Na}}$  is approximately 0.4  $\text{NPP}_K$ , and  $\text{NPP}_{\text{Cl}}$  is approximately  $10^4$ -fold  $\text{NPP}_K$ . The default parameter values used for  $H_{\max}$  and  $\text{NPP}_{K-\max}$  were 70% of the total initial Hb content of the host cell<sup>2</sup> and  $1.1 \text{ h}^{-1}$ ,<sup>15</sup> respectively. Half-time values were 32 hours and 27 hours for the H and  $\text{NPP}_K$  functions, respectively, and s was 3 hours for both functions.

Hb is incorporated within the parasite by endocytosis of the host cytoplasm.<sup>1,25</sup> Parasite volume growth is thus tightly linked to Hb digestion as follows. To digest the amount of Hb prescribed by the Y(H) function for any infinitesimal time interval (dt) the parasite would have to endocytose a volume of red cell cytoplasm ( $dV'$ ) that contains the required amount of Hb at the concentration prevailing in the host during dt. So, for each dt, the model reduces the host cell volume by  $dV'$  and increases parasite volume by  $dV'$ . Thus, parasite volume is computed at each stage as the cumulative sum of all the  $dV'$ 's up to that stage. Within each dt, the total change in host cell volume ( $dV$ ) will be given by the algebraic sum of  $dV'$  and of all osmotically driven fluid transfers ( $dV''$ ). Thus,  $dV = dV' + dV''$ . With this strategy, parasite volume growth is determined by the Hb consumption function, whereas the volume changes within the host compartment are additionally determined by all passive and active fluxes across the host cell plasma membrane. Note that  $dV''$  and  $dV'$  are interdependent quantities: fluid transfers determine the  $dV'$ , which contains the prescribed amount of Hb to be digested within dt, and, in turn,  $dV''$  is influenced by host residual volume and Hb content. At each time (t), parasite volume ( $V_P$ ) and host cell volume ( $V_H$ ) are computed from  $V_P = V_P^0 + \sum dV'$  and  $V_H = V_H^0 + \sum dV'' - \sum dV'$ , respectively, where  $V_P^0$  represents the initial postinfection parasite volume, assumed to be 4 fL, and  $V_H^0$  represents the initial host cell volume, normalized to 1. IRBC volume ( $V_{\text{IRBC}}$ ) is defined by  $V_{\text{IRBC}} = V_H + V_P$ . The predicted normalized values of  $V_{\text{IRBC}}$ ,  $V_H$ , and  $V_P$ , using default parameter values, are reported in Figure 2C for the complete asexual cycle (below). At 30 to 34 hours after invasion, predicted  $V_P$  falls within the range of 18 to 32 fL; by 48 hours,  $V_P$  reaches about 80% of the initial red cell volume, about 70 fL, equivalent to the volume occupied by approximately 16 new merozoites and the residual body. These values correlate well with previously measured mean trophozoite volumes of 20 to 28 fL<sup>26-28</sup> and with mean merozoite yields. The critical hemolytic volume of the IRBC was set at the mean relative cell volume (RCV) of 1.7,<sup>29</sup> equivalent to about 150 fL per cell, on the assumption, supported by early results of Nash et al,<sup>30</sup> that there are no major changes in the membrane area of the host red cell.

An important assumption in this modeling strategy is that the homeostatic behavior of the host cell is influenced mainly through NPP induction and  $dV$  feeds. Solute exchanges between parasite and host, as well as many of the other red cell membrane alterations induced by the parasite may be important for specific roles in parasite and host, but, within current knowledge, their relevance to IRBC homeostasis is not apparent.

## Results

The stage-dependent patterns of Hb digestion and of NPP-mediated permeabilities were derived from recently published data<sup>2,15</sup> and encoded in the model as shown in Figure 1 and detailed in "Materials and methods." The curves approach maximal values of  $\text{NPP}_{K-\max}$ , representing the maximal NPP-mediated  $\text{K}^+$  flux, and of  $H_{\max}$ , representing the maximal fraction of host Hb consumed. Parasite volume growth is determined by the Hb consumption curve, as explained in "Materials and methods."

The time-dependent patterns in Figure 1 describe 3 stages in host permeabilization and Hb consumption: a long latency during the ring stage, a rapid exponential rise starting at the young trophozoite stage, and a leveling-off phase through to schizont and segmentor stages. This time-dependent pattern parallels other growth and metabolic activities of the parasite.<sup>31-34</sup>

Figure 2 shows the changes in the main homeostatic variables of IRBCs predicted by the HCM. The model reproduced the known patterns of change in the  $\text{Na}^+$ ,  $\text{K}^+$ , and Hb content of host red cells<sup>2,14</sup> (Figure 2A-B). The critical novel predictions concerned the stage-related volume changes of parasite and host cells shown in Figure 2C. Unlike with uninfected red cells,<sup>15</sup> the model predicted that NPP-permeabilization and parasite volume growth would not

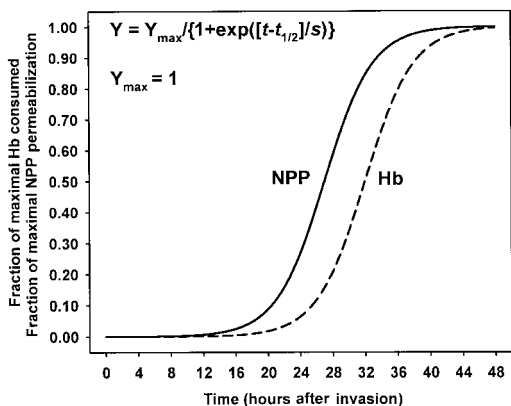


**Figure 1.** Time courses of NPP induction and Hb consumption by *P falciparum* parasites during their 48-hour asexual reproduction cycle in human red cell hosts as encoded in the homeostatic model of IRBCs. The curves follow the equation given in the figure. They represent the patterns observed by Staines et al<sup>15</sup> for  $Y = \text{NPP}_K$  and by Krugliak et al<sup>2</sup> for  $Y = \text{Hb}$  (or H), and are shown in the figure normalized to maximal values of 1. The default parameter values used in the model and in the simulations of Figures 2 and 5 (unless specified otherwise) were for  $Y = \text{NPP}_K$ ,  $\text{NPP}_{K\text{-max}} = 1.1 \text{ h}^{-1}$ ,  $t_{1/2} = 27$  hours and  $s = 3$ , and for  $Y = \text{H}$ ,  $H_{\text{max}} = 70\%$ ,  $t_{1/2} = 32$  hours and  $s = 3$ . These values compare with those measured as follows: for  $\text{NPP}_K$ ,  $t_{1/2} =$  approximately 27 hours, and  $\text{NPP}_{K\text{-max}} =$  approximately  $1 \text{ h}^{-1}$  (Staines et al<sup>15</sup>; estimated from their Figures 2 and 7); for H,  $t_{1/2} =$  approximately 32 hours, and  $H_{\text{max}} = 65\%$  (Krugliak et al<sup>2</sup>; estimated by combining data from their Figures 2, 3, and 4).

induce the hemolysis of IRBCs by the end of the 48-hour asexual cycle.

According to the model, IRBC volume would change little before NPP development. As NPP-mediated permeability increases, and coincidental with the highest rate of  $\text{Na}^+$  and  $\text{K}^+$  gradient dissipation (Figure 2A), excess  $\text{KCl}$  loss over  $\text{NaCl}$  gain would cause transient shrinkage, as expected from a  $P_K/P_{\text{Na}}$  permeability ratio of about 2.3<sup>15</sup> and from the high initial outward  $\text{K}^+$  gradient across the RBC plasma membrane. After the initial  $\text{K}^+$  and  $\text{Na}^+$  gradient dissipation, the inward colloid osmotic gradients would drive  $\text{NaCl}$  and water in swelling the cells toward a volume lower than the critical hemolytic volume by 48 hours, with a small but significant safety margin for additional swelling (Figure 2C). The model predicts distinct contributions of parasite and host cell to the overall volume change of IRBCs. Whereas parasite volume increases monotonically, the predicted host cell volume displays a clear wavy pattern after about 16 hours after invasion (Figure 2C), with 4 distinct phases: (1) initial shrinkage due to  $\text{KCl}$  loss exceeding  $\text{NaCl}$  gain through developing NPPs, (2) swelling due to sustained net  $\text{NaCl}$  and water gain after  $\text{K}^+$  gradient dissipation, (3) volume reduction due to transfers of cytoplasm from host to parasite exceeding swelling tendency from net  $\text{NaCl}$  gain; during this period, dilution of Hb in the host cell (Figure 2B) imposes larger  $dV'$  parasite feeds to incorporate the amounts of Hb prescribed by the  $Y(\text{H})$  function (“Materials and methods”), and (4) a final stage in which net  $\text{NaCl}$  gain and colloid osmotic swelling prevail again over declining parasite growth. By 48 hours, host cell volume is reduced to about 80% of its original value, and parasite volume exceeds that of the host cell (Figure 2C).

Before any further analysis of the factors, which according to the model ensure the integrity of the infected cell to the end of the parasite reproduction cycle, it was essential to seek experimental confirmation of the volume changes predicted in Figure 2C to establish the reliability of the model for the interpretation of the homeostatic behavior of IRBCs.

The volume changes predicted by the model were tested by comparing the osmotic fragility distribution of IRBC populations

with that of coincubated, mostly uninfected red cells (cohorts; “Materials and methods”). If the volume of IRBCs changes as predicted by the model (Figure 2C), then the osmotic fragility of IRBCs would be expected to vary little from controls during the first 16 to 20 hours of the parasite’s asexual cycle, to decrease slightly around 24 hours after invasion (late rings to young trophozoites) when IRBC volume is somewhat reduced, and to increase steadily from about 26 to 28 hours onwards (through mature trophozoite, schizont, and segmentor stages). These osmotic fragility changes were followed by comparing hemolysis curves from cohorts (controls) with those of concentrated IRBCs obtained from unsynchronized and synchronized cultures. IRBCs with young trophozoites would require more water gain than control cells to reach their critical hemolytic volume, whereas little extra swelling would be required to bring IRBCs with schizonts or segmentors to their critical hemolytic volume. This could easily be detected as left or right shifts in the hemolysis curves of IRBCs relative to those of cohorts, respectively. Hemolysis curves of IRBCs from unsynchronized cultures may be expected to show both left and right shifts with the crossover points determined by

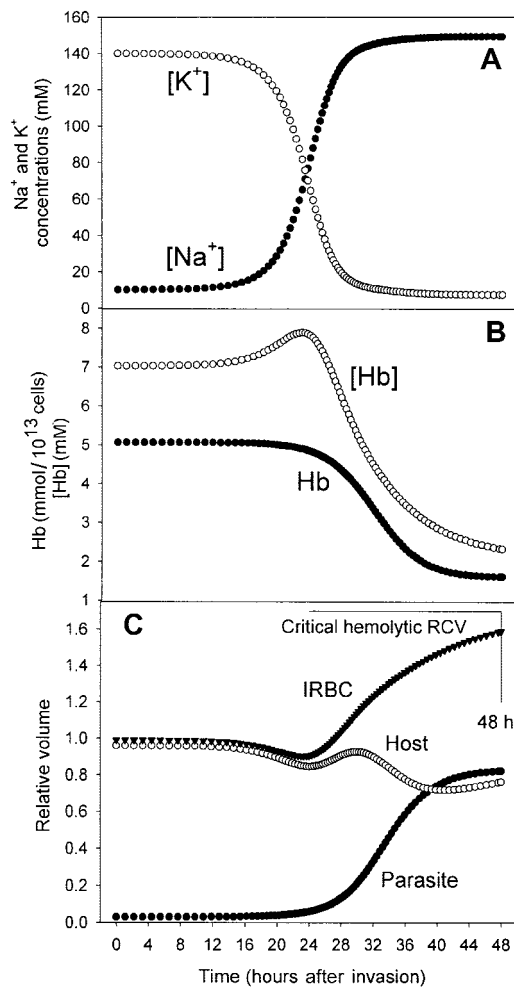


**Figure 2.** Predicted changes in selected homeostatic variables of *P falciparum*-infected red cells during the asexual reproduction cycle of the parasite. The panels show the predicted changes in (A) host cell  $\text{Na}^+$  and  $\text{K}^+$  concentrations and (B) Hb content (Hb) and concentration ( $[\text{Hb}]$ ); Hb content is expressed per  $10^{13}$  cells, the approximate number of cells contained in 1 liter of normal, uninfected human red cells. (C) Relative cell volume of IRBCs ( $\blacktriangledown$ ) and relative host ( $\circ$ ) and parasite ( $\bullet$ ) volumes; all volumes are expressed relative to RBC volume at the time of invasion, defined as 1. The horizontal top line in panel C indicates the mean critical hemolytic RCV,<sup>29</sup> and the vertical right hand line indicates the 48-hour end of the asexual cycle.

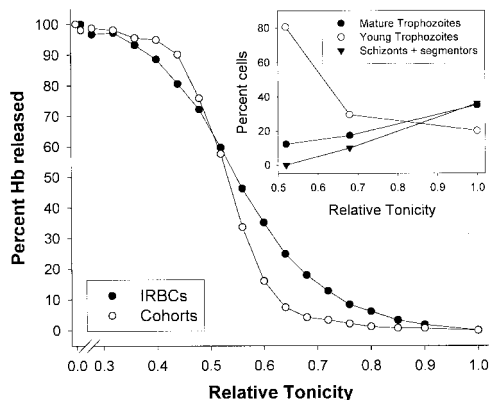


**Figure 3. Osmotic fragility curves of IRBCs and noninfected (cohorts) cells from the same *P falciparum* culture.** Hemolysis was induced by delivery of 10  $\mu$ L cell suspension (5% or 10% hematocrit) to each of 24 wells containing 250  $\mu$ L lysing media with different tonicities ("Materials and methods"). The lysing media were prepared by mixing 2 solutions: one containing 150 mM NaCl and 2 mM HEPES-Na, pH 7.5, equiosmolal with the culture medium used, regarded as relative tonicity (RT) = 1, and the other containing 2 mM HEPES-Na, pH 7.5, assumed equivalent to RT approximately 0. The experiment was performed on a nonsynchronized culture containing 18% parasitized cells. Separation of IRBCs and cohorts was done by gelatin flotation ("Materials and methods"). Parasitemia in IRBC and cohort fractions was 96% and 3.2%, respectively. Differential counts (500 cells) in IRBCs rendered 5% rings, 20% young trophozoites, 35% mature trophozoites, 36% schizonts plus segmentors, and 4% uninfected cells, whereas in the cohort fraction, 81% of the 3.2% IRBCs were rings. The y-axis reports percentage of Hb released by cell lysis. For cohorts, this is equivalent to percentage of cells lysed. For IRBCs, on the other hand, the Hb contribution from the cells with mature parasites is less than that from cells with younger parasites. Therefore, the right shift of the IRBC hemolysis curve relative to cohorts tends to underrepresent the true number of cells lysed. Inset: differential counts of unlysed IRBCs recovered from selected hemolysis wells ("Materials and methods"). After removal of residual lysis fluid, the cell pellets were resuspended in supplemented RPMI for smearing and staining. In all such recovered samples there was a variable abundance of lysed ghosts with stained parasite fragments. Differential counts (200 cells) were performed only on clearly recognizable intact cells. Differential counts were performed in 3 of the 6 experiments of this series in which crossover patterns were observed, with similar results to those shown in this inset.

the relative proportions of young and mature parasite forms, whereas curves of IRBCs from synchronized cultures would show mostly or exclusively left or right shifts depending on how well synchronized and at what stage they were.

Figure 3 reports the result of an experiment with IRBCs and cohorts from a nonsynchronized culture, representative of 6 with similar results. The figure shows the hemolysis curves of cells from top and bottom gelatin fractions containing 96% IRBCs and over 96% cohorts, respectively. The inset (Figure 3) reports the differential cell count in unlysed cells recovered from microplate wells with the relative tonicities (RTs) indicated in the figure ("Materials and methods").

It can be seen (Figure 3) that the hemolysis curve of the IRBCs is right-shifted at the higher tonicities and left-shifted at the lower tonicities, relative to the hemolysis curve of the cohorts. This pattern was reproduced in the 6 experiments of this series. The more mature the parasite population, the lower the RT at which the crossover occurred, as expected from the decline in the relative proportion of young trophozoites. Microscopic inspection of IRBCs that did not lyse in hypotonic media showed a consistent and clear tendency for the progressive decline in the proportion of mature parasite forms and enrichment in young trophozoites with decreasing tonicity (Figure 3, inset).

The results of Figure 3 are typical of IRBCs concentrated from nonsynchronized cultures. According to the model, IRBC samples containing only young trophozoites should show no right shift and those containing only mature trophozoites should show no left

crossover. This was tested in 3 additional experiments with IRBCs harvested from synchronized cultures, 1 containing only young trophozoites and 2 containing mature trophozoites, schizonts, and segmentors but no young parasite forms (Figure 4). It can be seen that IRBCs with young parasites showed no right shift, only a barely detectable, not statistically significant left shift (Figure 4A). It should be noted that in samples from highly synchronized cultures it may be more difficult to generate IRBC samples with parasites at a developmental stage precisely within the narrow 2- to 4-hour time period for which slight dehydration is predicted (Figure 2C) than in nonsynchronized cultures. Thus, absence of right shift is the only significant result in Figure 4A. On the other hand, only right shifts with no crossovers were obtained in samples of IRBCs containing only mature parasite forms (Figure 4B). Taken together, these results reveal a stage-related, gradually increasing osmotic fragility pattern, reflecting the continued volume expansion of IRBCs with mature parasites, consistent with the model predictions.

## Discussion

In the comparison between predicted and observed results, it is important to bear in mind the approximate nature of the model predictions. The model analyzes an oversimplified condition of identical red cells, defined by mean-valued parameters, invaded by single, identically developing parasites, whereas real IRBC populations, on which the predictions were tested, are highly heterogeneous in certain aspects relevant to volume homeostasis such as multiple invasion, intrinsic variations in membrane area, Hb content, and Hb concentration of invaded RBCs, and in the timing and extent of NPP and Hb consumption development among

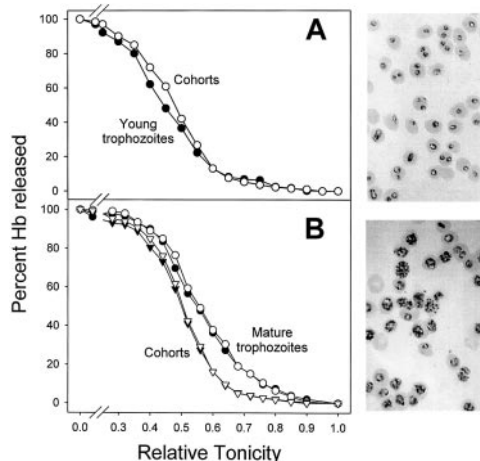


**Figure 4. Osmotic fragility curves of IRBCs obtained from synchronized *P falciparum* cultures.** The IRBCs contained either young (A) or mature (B) parasite forms. The osmotic fragility measurements were performed as described for Figure 3, using mostly uninfected cohort cells as controls. Synchronization was performed as described in "Materials and methods." Micrographs of representative fields from Giemsa-stained smears of the synchronized, concentrated cultures used for the osmotic fragility measurements are shown on the right of the corresponding figures (original magnification,  $\times 1000$ ). (A) A single experiment with culture containing rings and young trophozoite stage parasites. Top fraction ( $\bullet$ ): 91% parasitemia, all rings and young trophozoites. Bottom fraction ( $\circ$ ; cohorts): 94% uninfected cells, 6% rings. (B) Shown is 1 of 2 identical experiments with similar results. The culture contained mature stage trophozoites and 1.2% ring-stage parasites before final gelatin flotation. Top fraction ( $\bullet$ ,  $\circ$ ): 86% parasitemia, 33% mature trophozoites, and 53% schizonts and segmentors. Bottom fraction ( $\blacktriangledown$ ,  $\triangledown$ ): 97% uninfected cohorts and 3% rings.

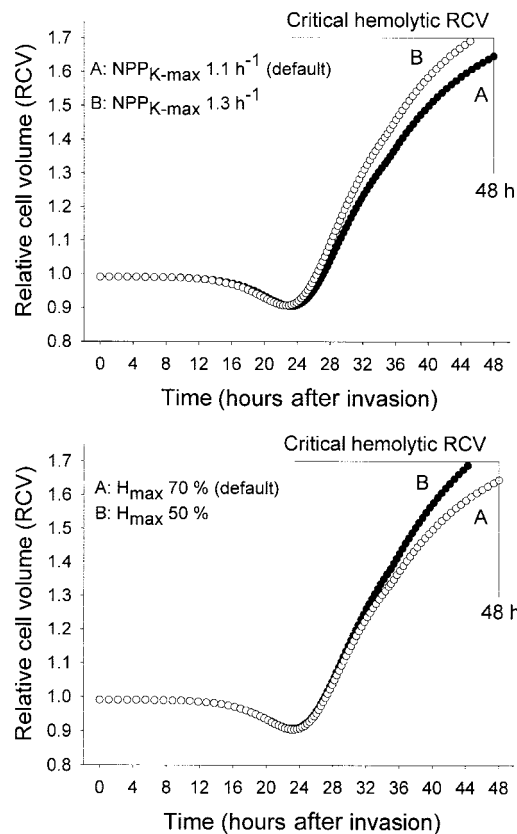


**Figure 5.** Effect of the magnitude of NPP-mediated permeabilization and of hemoglobin consumption on the predicted relative cell volume changes of parasitized red cells. In both panels, the curves predicted using the default parameter values for  $NPP_{K-max}$  and  $H_{max}$  (curves labeled A) are compared with those obtained using the slightly different values indicated for the curves labeled B. To incorporate the findings of Staines et al,<sup>15</sup> all simulations were performed with approximately 50% Na-pump inhibition after 35 hours. Comparison of Figure 2C with curve A, top panel of Figure 4, shows that the predicted volume changes with or without Na-pump inhibition were very similar. Note that the default values of  $NPP_{K-max}$  and  $H_{max}$ , based on the measured values of these parameters, are near the critical limits (shown as horizontal lines) required to preserve host cell integrity to the end of the asexual cycle.

parasites. Within these semiquantitative constraints, the results in Figures 3 and 4 do support the overall reliability of the volume predictions advanced in Figure 2C, and we can now ask how the model accounts for the volume stability of the infected cells.

To understand which are the main factors that prevent premature IRBC lysis, exploratory simulations were performed varying parameter values away from their experimentally based default values. The 2 most critical parameters for the understanding of host cell homeostasis proved to be  $NPP_{K-max}$  and  $H_{max}$ . Figure 5 shows the results of simulations in which these 2 parameters were varied alternatively. The effects on host cell volume of  $NPP_{K-max}$  values higher than those measured by Staines et al<sup>15</sup> are illustrated in Figure 5, top panel. It can be seen that the measured  $NPP_{K-max}$  permeability of  $1.1 \text{ h}^{-1}$  is very near the maximal value compatible with host viability. With a slightly higher value of  $1.3 \text{ h}^{-1}$  the HCM

predicts premature host lysis. The population distributions of Hb contents and critical hemolytic volumes in normal human red cells have coefficients of variation of about 13% and 6%, respectively.<sup>22</sup> Model simulations within 2 standard deviation boundaries of these variables indicated that host cell integrity at 48 hours after invasion would be compromised in more than 95% of IRBCs if  $NPP_{K-max}$  values exceeded  $1.8 \text{ h}^{-1}$  ( $H_{max}$  set at about 60%-70%).

Figure 5, bottom panel, illustrates the predicted effects of reduced Hb consumption on host cell volume. Model simulations using  $H_{max}$  values lower than those measured by Krugliak et al,<sup>2</sup> exemplified by the curve with 50%  $H_{max}$ , predict early host lysis. Thus, integrity of IRBCs by 48 hours requires a sustained and substantial decline in the concentration of Hb, to reduce the colloid osmotic pressure and consequently the rate of swelling of the permeabilized host cell.

These results provide a novel insight into the significance of the  $NPP_{K-max}$  value measured by Staines et al<sup>15</sup> suggesting that  $NPP_{K-max}$  represents a finely tuned compromise between the need to ensure an optimal traffic route for nutrient and waste product transport<sup>6</sup> and the need to preserve the osmotic integrity of the host to the end of the asexual reproduction cycle, with a reasonable safety margin. Could osmotic swelling determine the timing of rupture and merozoite release? In all the experiments of this series no significant lysis was observed until the relative tonicity was reduced lower than 0.9 (Figures 3 and 4B), in broad agreement with the predicted safety margin of about 0.94 ( $1.6/1.7$ ; Figures 2C, 5). Therefore, it is unlikely that osmotic effects could play any part in the process of rupture.

At face value, the prediction that reduced Hb consumption could cause premature host cell lysis (Figure 5) may appear counterintuitive and surprising. After dissipation of the  $\text{Na}^+/\text{K}^+$  gradients, the main driving force for IRBC swelling is the colloid osmotic pressure exerted by the impermeant solutes, mostly Hb, in the host cell cytoplasm. A high residual Hb would therefore speed up swelling of the host toward early lysis. The predictions in Figure 5, bearing in mind their approximate nature as discussed above, indicate that for the observed value of  $NPP_{K-max}$ , premature hemolysis of IRBCs can be prevented only if the Hb content of the host is reduced by more than 50%.  $NPP_{K-max}$  and  $H_{max}$  are linked in the preservation of IRBC integrity: the lower  $NPP_{K-max}$ , the lower the need to consume excess Hb. The evolutionary pressures that set the observed values of  $NPP_{K-max}$  and  $H_{max}$  suggest that the need to ensure high nutrient and waste traffic via NPPs took priority over the energy investments required for host cell ingestion and digestion and to prevent ferriprotoporphyrin IX-induced damage. In conclusion, the high measured values of  $NPP_{K-max}$  make excess hemoglobin consumption necessary to ensure the osmotic stability of IRBCs throughout the asexual reproduction cycle of the parasite.

## Acknowledgments

We are grateful to the Wellcome Trust, United Kingdom, for funds, and to Mrs Lynn Macdonald for excellent technical assistance.

## References

- Rudzinska MA, Trager W, Bray RS. Pinocytotic uptake and the digestion of hemoglobin in malaria parasites. *J Protozool.* 1965;12:563-576.
- Krugliak M, Zhang J, Ginsburg H. Intraerythrocytic *Plasmodium falciparum* utilizes only a fraction of the amino acids derived from the digestion of host cell cytosol for the biosynthesis of its proteins. *Mol Biochem Parasitol.* 2002;119:249-256.
- Zarchin S, Krugliak M, Ginsburg H. Digestion of the host erythrocyte by malaria parasites is the primary target for quinoline-containing antimalarials. *Biochem Pharmacol.* 1986;35:2435-2442.
- Kutner S, Breuer WV, Ginsburg H, Aley SB, Cabantchik ZI. Characterization of permeation pathways in the plasma membrane of human

- erythrocytes infected with early stages of *Plasmodium falciparum*: association with parasite development. *J Cell Physiol*. 1985;125:521-527.
5. Ginsburg H, Kutner S, Krugliak M, Cabantchik ZI. Characterization of permeation pathways appearing in the host membrane of *Plasmodium falciparum* infected red blood cells. *Mol Biochem Parasitol*. 1985;14:313-322.
  6. Kirk K. Membrane transport in the malaria-infected erythrocyte. *Physiol Rev*. 2001;81:495-537.
  7. Trager W. Digestion and indigestion in malaria parasites. *J Clin Invest*. 1994;93:1353.
  8. Aikawa M, Huff CG, Sprinz H. Fine structure of the asexual stages of *Plasmodium elongatum*. *J Cell Biol*. 1967;34:229-249.
  9. Sullivan DJ Jr, Gluzman IY, Goldberg DE. Plasmodium hemozoin formation mediated by histidine-rich proteins. *Science*. 1996;271:219-222.
  10. Francis SE, Sullivan DJ, Goldberg DE. Hemoglobin metabolism in the malaria parasite *Plasmodium falciparum*. *Annu Rev Microbiol*. 1997;51:97-123.
  11. Orjih AU, Banyal HS, Chevli R, Fitch CD. Hemin lyses malaria parasites. *Science*. 1981;214:667-669.
  12. Ridley RG, Dorn A, Vippagunta SR, Vennerstrom JL. Haematin (haem) polymerization and its inhibition by quinoline antimalarials. *Ann Trop Med Parasitol*. 1997;91:559-566.
  13. Ginsburg H, Ward SA, Bray PG. An integrated model of chloroquine action. *Parasitol Today*. 1999;15:357-360.
  14. Lee P, Ye Z, Van Dyke K, Kirk RG. X-ray microanalysis of *Plasmodium falciparum* and infected red blood cells: effects of qinghaosu and chloroquine on potassium, sodium, and phosphorus composition. *Am J Trop Med Hyg*. 1988;39:157-165.
  15. Staines HM, Ellory JC, Kirk K. Perturbation of the pump-leak balance for Na<sup>+</sup> and K<sup>+</sup> in malaria-infected erythrocytes. *Am J Physiol Cell Physiol*. 2001;280:C1576-C1587.
  16. Berendt AR, Simmons DL, Tansey J, Newbold CI, Marsh K. Intercellular adhesion molecule-1 is an endothelial cell adhesion receptor for *Plasmodium falciparum*. *Nature*. 1989;341:57-59.
  17. Trager W, Jensen JB. Human malaria parasites in continuous culture. *Science*. 1976;193:673-675.
  18. Lambros C, Vanderberg JP. Synchronization of *Plasmodium falciparum* erythrocytic stages in culture. *J Parasitol*. 1979;65:418-420.
  19. Jensen JB. Concentration from continuous culture of erythrocytes infected with trophozoites and schizonts of *Plasmodium falciparum*. *Am J Trop Med Hyg*. 1978;27:1274-1276.
  20. Pasvol G, Wilson RJM, Smalley ME, Brown J. Separation of viable schizont-infected red cells of *Plasmodium falciparum* from human blood. *Ann Trop Med Parasitol*. 1978;72:87-88.
  21. Tiffert T, Ginsburg H, Krugliak M, Elford BC, Lew VL. Potent antimalarial effects of clotrimazole in *in vitro* cultures of *Plasmodium falciparum*. *Proc Natl Acad Sci U S A*. 2000;97:331-336.
  22. Lew VL, Raftos JE, Sorette MP, Bookchin RM, Mohandas N. Generation of normal human red cell volume, hemoglobin content and membrane area distributions, by "birth" or regulation? *Blood*. 1995;86:334-341.
  23. Lew VL, Bookchin RM. Volume, pH and ion content regulation in human red cells: analysis of transient behavior with an integrated model. *J Membr Biol*. 1986;92:57-74.
  24. Kirk K, Horner HA, Elford BC, Ellory JC, Newbold CI. Transport of diverse substrates into malaria-infected erythrocytes via a pathway showing functional characteristics of a chloride channel. *J Biol Chem*. 1994;269:3339-3347.
  25. Yayon A, Timberg R, Friedman S, Ginsburg H. Effects of chloroquine on the feeding mechanism of the intraerythrocytic human malarial parasite *Plasmodium falciparum*. *J Protozool*. 1984;31:367-372.
  26. Elliott JL, Saliba KJ, Kirk K. Transport of lactate and pyruvate in the intraerythrocytic malaria parasite, *Plasmodium falciparum*. *Biochem J*. 2001;355:733-739.
  27. Saliba KJ, Kirk K. H<sup>+</sup>-coupled pantothenate transport in the intracellular malaria parasite. *J Biol Chem*. 2001;276:18115-18121.
  28. Saliba KJ, Horner HA, Kirk K. Transport and metabolism of the essential vitamin pantothenic acid in human erythrocytes infected with the malaria parasite *Plasmodium falciparum*. *J Biol Chem*. 1998;273:10190-10195.
  29. Ponder E. Hemolysis and Related Phenomena. New York, NY: Grune & Stratton; 1948.
  30. Nash GB, O'Brien E, Gordon-Smith EC, Dormandy JA. Abnormalities in the mechanical properties of red blood cells caused by *Plasmodium falciparum*. *Blood*. 1989;74:855-861.
  31. Krungkrai SR, Suraveratun N, Rochanakij S, Krungkrai J. Characterisation of carbonic anhydrase in *Plasmodium falciparum*. *Int J Parasitol*. 2001;31:661-668.
  32. Srivastava P, Pandey VC. Heme synthesizing enzymes of *Plasmodium knowlesi*: a simian malaria parasite. *Exp Parasitol*. 1998;88:60-63.
  33. Srivastava IK, Schmidt M, Grall M, Certa U, Garcia AM, Perrin LH. Identification and purification of glucose phosphate isomerase of *Plasmodium falciparum*. *Mol Biochem Parasitol*. 1992;54:153-164.
  34. Pfaller MA, Krogstad DJ, Parquette AR. *Plasmodium falciparum*: stage-specific lactate production in synchronized cultures. *Exp Parasitol*. 1982;54:391-396.